Rough and smooth variant *Mycobacterium abscessus* infections are differentially controlled by host immunity during chronic infection of adult zebrafish

Elinor Hortle[1,2]*, Julia Y Kam[1]*, Elizabeth Krogman[1]*, Sherridan E Warner[1,2], Pradeep Manuneedhi Cholan[1], Kazu Kikuchi[3,4], James A Triccas[2], Warwick J Britton[1,2], Matt D Johansen[5], Laurent Kremer[5,6], Stefan H Oehlers[1,2#]

1 Tuberculosis Research Program at the Centenary Institute, The University of Sydney, Camperdown NSW Australia

2 The University of Sydney, Faculty of Medicine and Health & Marie Bashir Institute, Camperdown NSW Australia

3 Developmental and Stem Cell Biology Division, Victor Chang Cardiac Research Institute, Darlinghurst, NSW Australia

4 St. Vincent's Clinical School, University of New South Wales, Kensington, NSW 2052, Australia

5 Centre National de la Recherche Scientifique UMR 9004, Institut de Recherche en Infectiologie de Montpellier (IRIM), Université de Montpellier, 1919 Route de Mende, 34293, Montpellier, France.

6 INSERM, IRIM, 34293 Montpellier, France.

*These authors contributed equally and are listed in alphabetical order.

[#] Corresponding author: Dr Stefan Oehlers, stefan.oehlers@sydney.edu.au

Author contributions

EH: qPCR analyses; JK: histological analysis; EK: dose finding, survival experiments, histological analysis; SW: CFU recovery assays; PMC: histological analysis; KK: provided reagents; JAT & WJB: supervision of study; MDJ: conceived study, supervision of study, wrote manuscript; LK: conceived study, provided reagents, supervision of study, wrote manuscript; SHO: conceived study, performed experiments, supervision of study, wrote manuscript.

Keywords: non-tuberculous mycobacterium, rapid-growing mycobacteria, animal model, zebrafish, glycopeptidolipids

Abstract

Infections caused by *Mycobacterium abscessus* are increasing in prevalence within patient groups with respiratory comorbidities including Cystic Fibrosis or Chronic Obstructive Pulmonary Disease. Initial colonisation by the smooth colony *M. abscessus* (S) can be followed by an irreversible genetic switch into a highly inflammatory rough colony *M. abscessus* (R), often associated with a decline in pulmonary function. Currently available animal models such as the embryonic zebrafish, have largely explored the role of innate immunity in the pathogenesis of *M. abscessus*, and demonstrated that infection with the R variant produces a hyperinflammatory infection due to the presence of large extracellular cords, whereas the S variant produces a chronic persistent infection. However, our understanding of the role of adaptive immunity in *M. abscessus* pathogenesis is largely unknown. Here, we have used intraperitoneal infection of adult zebrafish to model *M. abscessus* pathogenesis in the context of fully functioning host immunity. We find infection with the R variant penetrates host organs causing an inflammatory immune response leading to necrotic granuloma and abscess formation within 2 weeks. The R bacilli are targeted by T cell-mediated immunity and burden is progressively reduced. Strikingly, the S variant colonises host internal surfaces at high loads and is met with a robust innate immune response but little T cell-mediated immunity. Invasive granuloma formation is delayed in S variant infection compared to R variant infection upon which T cell-mediated immunity is required to control infection. In mixed infections, the S variant outcompetes the R variant in an adaptive-immunity dependent manner. We also find the R variant activates innate immunity to detriment of S variant *M. abscessus* in mixed infections. These findings demonstrate the applicability of the adult zebrafish to model persistent *M. abscessus* infection and provide insight into the immunopathogenesis of chronic *M. abscessus* infection.

Introduction

Mycobacterium abscessus is an increasingly recognized human pathogen responsible for a wide array of clinical manifestations including muco-cutaneous infections, disseminated or chronic pulmonary diseases. The latter is mostly encountered in patients with underlying lung disorders, such as bronchiectasis or cystic fibrosis (CF). Irrespective of being a rapid-growing mycobacteria (RGM), *M. abscessus* displays many pathophysiological traits with slow-growing mycobacteria (SGM), such as *Mycobacterium tuberculosis*. These include the capacity to persist silently within granulomatous structures and to produce pulmonary caseous lesions (1, 2). In addition, *M. abscessus* is notorious for being one of the most-drug resistant mycobacterial species, characterized by a wide panel of acquired and innate drug resistance mechanisms against nearly all anti-tubercular drugs, as well as many classes of antibiotics (3). Consequently, this explains the complexity and duration of the treatments and the high level of therapeutic failure (4).

M. abscessus exists either as smooth (S) or a rough (R) colony morphotype variants associated with distinct clinical outcomes (5). Previous epidemiological studies have highlighted the association of the R variant, persisting for many years in the infected host, with a rapid decline in the pulmonary functions (6-8). It is well established that these morphological differences between S and R variants are dependent on the presence or absence of surface-exposed glycopeptidolipids (GPL), respectively (5, 9, 10). However, our knowledge of the pathophysiological characteristics and interactions between R or S variants with the host immune cells remains largely incomplete and is hampered by the lack of animal models that are permissive to persistent *M. abscessus* infection.

Intravenous injection or aerosol administration of *M. abscessus* in immunocompetent BALB/c mice fails to establish a persistent infection, typified by a rapid clearance of the bacilli from the liver, spleen and lungs within 4 weeks (11). Immunosuppression is required to produce a progressive high level of infection with *M. abscessus* in mice, as shown in nude, SCID (severe combined immunodeficiency), interferon-gamma (GKO) and granulocyte-macrophage colony-stimulating factor (GM-CSF) knock-out mice (12).

The contribution of B and T cells in the control of *M. abscessus* infection has been studied in C57BL/6 mice with Rag2$^{-/-}$, Cd3e$^{-/-}$ and µMT$^{-/-}$ knockouts. These studies indicated that infection control was primarily T cell dependent in the spleen, and both B and T cell dependent in the liver (13). In addition, IFNg-receptor KO mice (ifngr1$^{-/-}$) were significantly impaired in their control of *M. abscessus* both in the spleen and in the liver, with markedly different granulomas and more pronounced in TNF$^{-/-}$ mice (13). This points to the central role of T-cell immunity, IFNg and TNF for the control of *M. abscessus* in C57BL/6 mice, similarly to the control of *M. tuberculosis* infection.

In recent years, alternative non-mammalian models, such as Drosophila (14), Galleria larvae (15), and zebrafish embryos (16) have been developed to study the chronology and pathology of *M. abscessus* infection and for *in vivo* therapeutic assessment of drugs active against *M. abscessus*. In particular, zebrafish embryos have delivered important insights into the pathogenesis of *M. abscessus* and the participation of innate immunity in controlling infection. The optical transparency of zebrafish embryos has been used to visualise the formation of large extracellular cords by the R form *in vivo*, representing a mechanism of immune subversion by preventing phagocytic destruction and highlighting the importance bacterial virulence factors such as the dehydratase MAB_4780 and the MmpL8$_{MAB}$ lipid transporter (9, 17, 18). Other studies in zebrafish embryos have demonstrated the contribution of host TNF signalling and IL8-mediated neutrophil recruitment for protective granulomatous immunity against *M. abscessus* (19), and the link between dysfunctional CFTR and vulnerability to *M. abscessus* infection via the macrophage oxidative response (20).

Adult zebrafish models have been well-described for the study of mycobacterial pathogenesis by *Mycobacterium marinum*, used as a surrogate for the closely related *M. tuberculosis*, and the human pathogen *Mycobacterium leprae* (21-23). Encompassing a fully functional immune system, previous studies in adult zebrafish with pathogenic mycobacteria such as *M. marinum* have unravelled the interplay between innate and adaptive immunity in mycobacterial granuloma formation and function.

Herein, we addressed whether adult zebrafish may be a useful host to analyse and compare the chronology of infection with *M. abscessus* S and R variants and to study the contribution of the T cell-mediated immunity and granulomatous response in *M. abscessus* infection.

Results

Adult zebrafish can be chronically infected with *M. abscessus.*

To establish the susceptibility of adult zebrafish to infection by *M. abscessus*, we performed a dose escalation experiment up to 10^6 CFU per animal with the rough (R) and smooth (S) variants of the reference strain CIP104536^T. While animals underwent a period of sickness behaviour within the first week of infection, we did not observe mortality for up to 4 weeks post infection (wpi) (data not shown). To determine if *M. abscessus* produces a persistent infection in adult zebrafish, we performed CFU recovery on animals infected with a standard dose of 10^5 CFU (Figure 1A). We observed a progressive clearance of the R variant with a 1-log reduction in burden from 1 day post infection (dpi) to 4 wpi (P=0.018). Conversely, the S variant was recovered at a consistent burden across the 4 week duration of the experiment (1 dpi vs 4 wpi, P=0.12).

Adult zebrafish mount a robust inflammatory response to *M. abscessus* infection.

We hypothesised that the better survival of the S variant compared to the R variant could be attributed to reduced immunogenicity of the CIP104536 S cell surface and differential modes of growth in macrophages (24). To test this hypothesis, we performed qPCR detection of zebrafish immune gene expression from whole body homogenates of infected animals (25). We observed higher innate immunity-associated *il1b* transcription in the *M. abscessus* S-infected group from early in infection and a late trend to increases in *il1b* transcription in 4 wpi *M. abscessus* R-infected animals indicating a stronger early innate immune response to the S variant (Figure 1B).

The cytokine *tumour necrosis factor* (*tnfa*) is essential for the granulomatous containment of *M. abscessus* in zebrafish embryos (19). There was a non-statistically significant trend to increased transcription of *tnfa* in whole body homogenates from animals infected with either variant of *M. abscessus* compared to uninfected animals (Figure 1C). We next took advantage of the *TgBAC(tnfa:GFP)*^{pd1028} zebrafish line (26), where GFP expression is driven by the *tnfa* promoter, to

investigate if *tnfa* expression is linked to granuloma formation. Expression of GFP was enhanced around either variant of *M. abscessus* and was tightly concentrated around organised granulomas demonstrating a conserved induction of *tnfa* expression during *M. abscessus* granuloma formation in adult zebrafish (Figure 1D and 1E).

Adult zebrafish contain *M. abscessus* R within granulomas.

We next performed histology on adult zebrafish infected with fluorescent *M. abscessus* R. At 3 dpi, bacteria were diffusely spread through the peritoneal cavity with occasional foci of infection located external to peritoneal organs. From 10 dpi to 2 wpi we noted a heterogeneous mix of unorganised lesions (Figure 2A) and organised lesions with stereotypical concentric rings of nuclei around a central focus of bacteria and necrotic debris in all animals (Figure 2B). We also observed the appearance of very large abscess-like granulomas filled with fluorescent bacteria and necrotic debris measuring over 600 µm at a rate of no more than 1 per infected animal from 2 wpi onwards (Figure 2C). Oil red O staining revealed the accumulation of foam cells in cellular rim of *M. abscessus* R granulomas (Figure 2D), consistent with immunopathology seen in immunocompromised mice infected with *M. abscessus* (12). Although we observed a fairly stable proportion of organised granulomas in *M. abscessus* R-infected adult zebrafish from 10 to 28 dpi (Figure 2E), the proportion of fluorescent bacteria associated with organised granulomas significantly increased from 10 to 28 dpi corresponding to the appearance of abscesses at 14 dpi (Figure 2F).

Adult zebrafish contain *M. abscessus* S infection prior to delayed granuloma formation.

Histological analysis of adult zebrafish infected with fluorescent *M. abscessus* S revealed significantly less tissue damage than the equivalent *M. abscessus* R infection up to 2 wpi. *M. abscessus* S was observed to grow freely in mesenteric spaces and form poorly organised cellular granulomas at 2 wpi (Figure 3A). We observed the appearance of tissue-invasive organised granulomas at 4 wpi (Figure 3B). Although these granulomas could reach similar size to the very large abscess-like granulomas seen in *M. abscessus* R infection, there was little Oil Red O staining in *M. abscessus* S granulomas indicating a lack of foam cell formation (Figure 3B).

We observed a significant increase in the proportion of organised granulomas in S-infected adult zebrafish from 2 to 4 wpi (Figure 3C). Similarly, the proportion of fluorescent bacteria associated with organised granulomas significantly also increased from 2 to 4 wpi corresponding to the consolidation of *M. abscessus* S into granulomas (Figure 3C).

Adaptive immunity differentially controls infection by *M. abscessus* variants in adult zebrafish.

Given the requirement for T cells to maintain granuloma structure in adult zebrafish *M. marinum* infection (23), we next asked if there was T cell involvement around *M. abscessus* granulomas using the recently described *TgBAC(lck:GFP)*^{vcc4} zebrafish line (23, 27). We observed T cell association and penetration throughout unorganised and organised *M. abscessus* R granulomas, but T cells were largely excluded from the cores of the very large abscess-like lesions (Figure 4A). Conversely, we did not observe T cell interaction with *M. abscessus* S growing around peritoneal organs until invasive granuloma formation after 2 wpi, which was indistinguishable from the T cell response to *M. abscessus* R infection (Figure 4B).

To directly test the requirement of T cells in containing *M. abscessus* we next utilised the *lck*$^{-/-sa410}$ mutant line which is T cell-deficient. We infected wild type (WT) control and *lck*$^{-/-sa410}$ mutant adult zebrafish with both the S and R variants. T cell-deficient adult zebrafish were significantly more susceptible to *M. abscessus* R infection with reduced survival over 4 weeks of infection (P = 0.0005, Log-rank test) (Figure 4C). T cell deficiency had a less pronounced effect on the survival of animals infected with *M. abscessus* S compared to *M. abscessus* R infection (WT S vs lck-/- S P = 0.03, Log-rank test), although both groups eventually succumbed to infection at the same rate after 5 wpi (P = 0.78, Log-rank test) (Figure 4C). Consequently, bacterial burden was significantly increased in 2 wpi *lck*$^{-/-sa410}$ mutants infected with the R (Figure 4D), but not the S variant (Figure 4E). These observations confirm the highly inflammatory nature of *M. abscessus* R infection is conserved in the adult zebrafish model and mediated by T-cells. Conversely, colonisation by *M. abscessus* S is contained by sufficient activation of the innate immune response until invasive infection between 2 and 4 wpi requires T-cell involvement to contain.

<u>*M. abscessus* S has a survival advantage over *M. abscessus* R.</u>

To examine our hypothesis that *M. abscessus* S has a survival advantage over *M. abscessus* R in the adult zebrafish infection model, we performed co-infection of adult zebrafish with equal numbers of each variant expressing either Wasabi or Tdtomato fluorescent proteins to enable simple tracking (Figure 5A). Analysis of the ratio of R:S colonies recovered revealed a clear and rapid shift in population proportions from 1:1 at 1 dpi to 0.5 rough:1 smooth ratio that remained stable at 2 wpi (Figure 5B). Coinfection did not affect the progressive reduction in *M. abscessus* R burden as near identical *M. abscessus* R CFUs were recovered from single and mixed-infected animals at 1 and 2 wpi (Figure 5C). Coinfection did cause a decrease in the number of recoverable *M. abscessus* S that was not observed in single variant infections at 1 and 2 wpi demonstrating a negative effect of R granuloma formation on the survival of *M. abscessus* S (Figure 5C). Whole mount and histological examination of bacterial distribution in animals infected with *M. abscessus* R expressing Wasabi

and *M. abscessus* S expressing Tdtomato revealed co-mingling of S and R variants within granulomas (Figure 5D).

We hypothesised that the T cell response induced by the R variant to antigens shared with the S variant could be responsible for the clearance of S variant in mixed infections. To test this hypothesis we infected T-cell deficient *lck*$^{-/-sa410}$ mutant animals with a mixed infection of R and S variants of *M. abscessus*. CFU recovery from these mixed infections in the T-cell deficient animals revealed a similar decrease in *M. abscessus* S burden as observed in WT animals (Figure 5E). Therefore the clearance of *M. abscessus* S variant is mediated by innate immune mechanisms. Interestingly, *lck*$^{-/-sa410}$ zebrafish had a higher proportion of rough to smooth than in comparable WT animals, confirming the importance of the adaptive immune response for controlling *M. abscessus* R variant burden (Figure 5F).

Discussion

In this study, we report for the use of adult zebrafish to probe both host and mycobacterial determinants of pathogenesis during persistent infection with *M. abscessus*. Infection with the R and S variants was maintained over months of infection in genetically intact animals, a major improvement on existing mouse models of *M. abscessus* infection.

While the R variant induces a more robust and aggressive infection than the S variant in zebrafish embryos (9), this appears to not the case in the adult fish. We observed better clearance of the R variant and establishment of a higher burden of persistent infection with the S variant. One possible explanation for the better survival of the S compared to the R is that, in the presence of effective adaptive immunity, R infection is better controlled due to the induction of a potent Th1 cell-mediated response, as evidenced by the increased expression of the CD3 marker and IFN-gamma response at later time points. This contribution of the T cell response was further substantiated using T cell-deficient fish, where infection of *lck*$^{-/-}$ fish with the R bacilli resulted in a higher bacterial burden than in WT fish, which was not observed with S bacilli. These observations provide insight into the clinical observation that AIDS patients are not at increased risk of *M. abscessus* infection to the same degree that AIDS is a risk factor for *M. tuberculosis* and other non-tuberculous mycobacterium infections such as *Mycobacterium avium*.

It is well known that the intracellular lifestyle of S and R *M. abscessus* variants differ significantly, resulting in entirely distinct infection scenarios (28). The absence of GPL on the outer mycomembrane causes corded growth of R variants, resulting in multiple bacilli being simultaneously phagocytosed by macrophages and overloaded phagosomes that rapidly activate autophagy pathways (28). Comparatively, the S variant is able to survive for an extended period of time within the phagosome, producing a chronic and persistent infection (29, 30). As such, these

polar infection responses may explain why the R displays increased granuloma formation at 2 wpi, compared to S which shows a significantly delayed onset of granuloma formation. Moreover, this observation matches the superior *in vivo* growth performance of S bacilli compared to R (Fig 1A), suggesting that the R variant is at an overall disadvantage because of its intrinsic hyper-inflammatory status and the activation of effective adaptive immunity that results in granuloma formation. Taken together, our data provides additional evidence for the distinct intracellular fates of both S and R variants *in vivo*, and further implicates the role of adaptive immunity in granuloma formation and control of *M. abscessus* infection in an adult zebrafish model.

Our qPCR analysis surprisingly demonstrated that the S variant elicits greater production of *il1b*; a key inflammatory cytokine, during the first 2 wpi compared to the R variant (Fig 1B). It is likely that this observation is the nett effect of progressive increase in bacterial burden of S variants over time, coupled with the presence of extracellular bacilli and unorganised granuloma formation observed at 2 wpi, compared to the containment and clearance of the R variant in organised granulomas.

T cells are critical host determinants in the control of mycobacterial infection (31). Recruitment of T cells into granulomas are thought to be essential in containing persistent infection, while T cell deficiencies are associated with greater mycobacterial infection severities (21, 31-33). Recently, an adult zebrafish infection model for *M. leprae* demonstrated that T cells are essential for containment of infection (30). We examined the recruitment of T cells within granulomas and identified that S variant granulomas were marked by the absence of T cell infiltration at 2 wpi, highlighting the fact that T cells may play a less significant role in S variant infections than those with R variants. Using the *lck*$^{-/-}$ mutants, we have shown that adult zebrafish are highly susceptible to *M. abscessus* infection and succumb to intraperitoneal infection within 40 days in the absence of T cells, irrespective of bacterial morphotype. Importantly, the R variant displayed an improved *in vivo* growth performance in the absence of T cells when compared to wild-type zebrafish, highlighting the role of T cells in the control of R variants. However, this observation was not maintained with the S variant, which showed no increase in bacterial growth *in vivo* irrespective of the absence of T cells early in infection.

Our co-infection experiments further support the theory that tissue destruction caused by R variant activates protective trans-acting host innate immunity that impairs bacterial growth, thereby restricting S growth. This suggests *M. abscessus* must balance the benefits of R variant pathogenicity allowing individuals to kill and escape macrophage containment, with the need to avoid activation of host-protective immunity at a population level.

To date, our understanding of the diverse immune responses between S and R variants have only been thoroughly described with respect to innate immunity, and currently our knowledge

pertaining to adaptive immunity in *M. abscessus* infection has been poorly characterised. Using this new adult zebrafish *M. abscessus* infection model, we have shown that S and R variants produce strikingly different disease phenotypes, which was further exemplified in the absence of a functioning adaptive immune response. Consequently, these results suggest that the host-pathogen interactions dictating *M. abscessus* pathogenesis are complex and may implicate adaptive immunity to a greater extent than originally anticipated. Future work should exploit this new animal model in combination with zebrafish lacking the Cystic fibrosis transmembrane conductance regulator gene, and for the development and testing of novel antibiotics and vaccine candidates that may be used for the treatment of *M. abscessus* infection.

Methods

Zebrafish strains and handling

Zebrafish strains used in this study are AB strain wildtype, *TgBAC(tnfa:GFP)*^{pd1028}, *TgBAC*(*lck*:*EGFP*)^{vcc4}, *lck-/-* ^{sa410} (26, 27). Animals were held in a 28°C incubator with a 14:10 hour light:dark cycle. Animals were infected by intraperitoneal injection with approximately 10^5 CFU *M. abscessus*, unless otherwise stated, using a 31 G insulin needle and syringe as previously described (34). Infected zebrafish were recovered into system water and held in 1 L beakers with daily feeding for the duration of the experiment. Infection experiments were carried out with ethical approval from the Sydney Local Health District Animal Welfare Committee approval 16-037.

M. abscessus strains and handling

Rough (R) and smooth (S) variants of *M. abscessus* strain CIP104536^T were grown at 30°C in Middlebrook 7H9 broth supplemented with 10% Oleic acid/Albumin/Dextrose/Catalase (OADC) enrichment and 0.05% Tween 80 or on Middlebrook 7H10 agar containing 10% OADC (7H10 OADC). Recombinant *M. abscessus* strains expressing Tdtomato or Wasabi were grown in the presence of 500 µg/ml hygromycin (9, 19). Homogenous bacterial suspensions for intraperitoneal injection in adult fish were prepared as previously reported (35).

Bacterial recovery

Animals were euthanised by tricaine anaesthetic overdose and rinsed in sterile water. Individual carcasses were homogenised and serially diluted into sterile water. Homogenates were plated onto 7H10 OADC supplemented with 300 µg/ml hygromycin. Plates were grown for at least 4 days at 37 degrees.

Zebrafish and *M. abscessus* gene expression analysis by qPCR

RNA was extracted from whole fish homogenates and was reverse transcribed with the Applied Biosystems High Capacity cDNA kit and qPCR was carried out on an Agilent Technologies Stratagene Mx3005P. Zebrafish gene expression primers were previously described by Hammaren *et al*. (25).

Histology

Animals subjected to cryosectioning as previously described (34). Briefly, euthanasia was performed by tricaine anaesthetic overdose and specimens were fixed for 2-4 days in 10% neutral buffered formalin at 4°. Specimens were then rinsed in PBS, incubated overnight in 30% sucrose, incubated overnight in 50/50 30% sucrose and OCT, and finally incubated overnight in OCT prior to freezing at -80°. Cryosectioning was performed to produce 20 µm thick sections. Sections were post-fixed for 1-2 minutes in 10% neutral buffered formalin and rinsed in PBS prior to further processing. Slides for fluorescent imaging were mounted with coverslips using Fluoromount G containing DAPI. Oil Red O staining was performed as previously described (34, 36). T cells were detected in sections from *TgBAC(lck:GFP)*^{vcc4} zebrafish by anti-GFP staining (primary antibody: ab13970, Abcam; secondary antibody: ab150173, Abcam), stained slides were then mounted with coverslips using Fluoromount G containing DAPI. All imaging was carried out on a Leica DM6000B microscope.

Statistics

All statistical testing was carried out using Graphpad Prism. Each data point indicates a single animal unless otherwise stated.

Acknowledgements

We thank the Centenary imaging facility core and Sydney Cytometry staff Drs Kristina Jahn, Angela Kurz, and David Liu, for their assistance.

Funding: Australian National Health and Medical Research Council CJ Martin Early Career Fellowship APP1053407 and Project Grant APP1099912; The University of Sydney Fellowship G197581; NSW Ministry of Health under the NSW Health Early-Mid Career Fellowships Scheme H18/31086; the Kenyon Family Foundation Inflammation Award; Australian-French Association for Research and Innovation (AFRAN) Initiative; The University of Sydney Marie Bashir Institute 2019 Seed Funding to SHO. Sydney Medical School Summer Scholarship to JYK. Post-doctoral fellowship granted by Labex EpiGenMed, an “Investissements d’avenir” program ANR-10-LABX-12-01 to MDJ. The Fondation pour la Recherche Médicale DEQ20150331719 to LK.

References

1. H. Medjahed, J. L. Gaillard, J. M. Reyrat, Mycobacterium abscessus: a new player in the mycobacterial field. *Trends Microbiol* **18**, 117-123 (2010).
2. J. F. Tomashefski, Jr., R. C. Stern, C. A. Demko, C. F. Doershuk, Nontuberculous mycobacteria in cystic fibrosis. An autopsy study. *Am J Respir Crit Care Med* **154**, 523-528 (1996).
3. R. Nessar, E. Cambau, J. M. Reyrat, A. Murray, B. Gicquel, Mycobacterium abscessus: a new antibiotic nightmare. *The Journal of antimicrobial chemotherapy* **67**, 810-818 (2012).
4. B. E. Ferro *et al.*, Failure of the Amikacin, Cefoxitin, and Clarithromycin Combination Regimen for Treating Pulmonary Mycobacterium abscessus Infection. *Antimicrob Agents Chemother* **60**, 6374-6376 (2016).
5. S. T. Howard *et al.*, Spontaneous reversion of Mycobacterium abscessus from a smooth to a rough morphotype is associated with reduced expression of glycopeptidolipid and reacquisition of an invasive phenotype. *Microbiology* **152**, 1581-1590 (2006).
6. E. Catherinot *et al.*, Acute respiratory failure involving an R variant of Mycobacterium abscessus. *J Clin Microbiol* **47**, 271-274 (2009).
7. C. R. Esther, Jr., D. A. Esserman, P. Gilligan, A. Kerr, P. G. Noone, Chronic Mycobacterium abscessus infection and lung function decline in cystic fibrosis. *J Cyst Fibros* **9**, 117-123 (2010).
8. B. E. Jonsson *et al.*, Molecular epidemiology of Mycobacterium abscessus, with focus on cystic fibrosis. *J Clin Microbiol* **45**, 1497-1504 (2007).
9. A. Bernut *et al.*, Mycobacterium abscessus cording prevents phagocytosis and promotes abscess formation. *Proc Natl Acad Sci U S A* **111**, E943-952 (2014).
10. H. Medjahed, J. M. Reyrat, Construction of Mycobacterium abscessus defined glycopeptidolipid mutants: comparison of genetic tools. *Appl Environ Microbiol* **75**, 1331-1338 (2009).
11. A. Bernut *et al.*, In vivo assessment of drug efficacy against Mycobacterium abscessus using the embryonic zebrafish test system. *Antimicrob Agents Chemother* **58**, 4054-4063 (2014).
12. A. Obregon-Henao *et al.*, Susceptibility of Mycobacterium abscessus to antimycobacterial drugs in preclinical models. *Antimicrob Agents Chemother* **59**, 6904-6912 (2015).
13. M. Rottman *et al.*, Importance of T cells, gamma interferon, and tumor necrosis factor in immune control of the rapid grower Mycobacterium abscessus in C57BL/6 mice. *Infect Immun* **75**, 5898-5907 (2007).
14. C. T. Oh, C. Moon, M. S. Jeong, S. H. Kwon, J. Jang, Drosophila melanogaster model for Mycobacterium abscessus infection. *Microbes Infect* **15**, 788-795 (2013).

15. M. Meir, T. Grosfeld, D. Barkan, Establishment and Validation of Galleria mellonella as a Novel Model Organism To Study Mycobacterium abscessus Infection, Pathogenesis, and Treatment. *Antimicrob Agents Chemother* **62** (2018).
16. A. Bernut, J. L. Herrmann, D. Ordway, L. Kremer, The Diverse Cellular and Animal Models to Decipher the Physiopathological Traits of Mycobacterium abscessus Infection. *Front Cell Infect Microbiol* **7**, 100 (2017).
17. V. Dubois *et al.*, MmpL8MAB controls Mycobacterium abscessus virulence and production of a previously unknown glycolipid family. *Proc Natl Acad Sci U S A* **115**, E10147-E10156 (2018).
18. I. Halloum *et al.*, Deletion of a dehydratase important for intracellular growth and cording renders rough Mycobacterium abscessus avirulent. *Proc Natl Acad Sci U S A* **113**, E4228-4237 (2016).
19. A. Bernut *et al.*, Mycobacterium abscessus-Induced Granuloma Formation Is Strictly Dependent on TNF Signaling and Neutrophil Trafficking. *PLoS Pathog* **12**, e1005986 (2016).
20. A. Bernut *et al.*, CFTR Protects against Mycobacterium abscessus Infection by Fine-Tuning Host Oxidative Defenses. *Cell reports* **26**, 1828-1840 e1824 (2019).
21. C. A. Madigan, J. Cameron, L. Ramakrishnan, A Zebrafish Model of Mycobacterium leprae Granulomatous Infection. *J Infect Dis* **216**, 776-779 (2017).
22. S. H. Oehlers *et al.*, Interception of host angiogenic signalling limits mycobacterial growth. *Nature* **517**, 612-615 (2015).
23. L. E. Swaim *et al.*, Mycobacterium marinum infection of adult zebrafish causes caseating granulomatous tuberculosis and is moderated by adaptive immunity. *Infect Immun* **74**, 6108-6117 (2006).
24. A. L. Roux *et al.*, The distinct fate of smooth and rough Mycobacterium abscessus variants inside macrophages. *Open Biol* **6** (2016).
25. M. M. Hammaren *et al.*, Adequate th2-type response associates with restricted bacterial growth in latent mycobacterial infection of zebrafish. *PLoS Pathog* **10**, e1004190 (2014).
26. L. Marjoram *et al.*, Epigenetic control of intestinal barrier function and inflammation in zebrafish. *Proc Natl Acad Sci U S A* **112**, 2770-2775 (2015).
27. K. Sugimoto, S. P. Hui, D. Z. Sheng, M. Nakayama, K. Kikuchi, Zebrafish FOXP3 is required for the maintenance of immune tolerance. *Dev Comp Immunol* **73**, 156-162 (2017).
28. A.-L. Roux *et al.*, The distinct fate of smooth and rough Mycobacterium abscessus variants inside macrophages. *Open biology* **6** (2016).
29. A. Bernut *et al.*, *Mycobacterium abscessus* cording prevents phagocytosis and promotes abscess formation. *Proceedings of the National Academy of Sciences* **111**, 943-952 (2014).

30. L. Ramakrishnan, Revisiting the role of the granuloma in tuberculosis. *Nature Reviews Immunology* **12**, 352-366 (2012).
31. F. M. Collins, Mycobacterial disease, immunosuppression, and acquired immunodeficiency syndrome. *Clin Microbiol Rev* **2**, 360-377 (1989).
32. T. Mogues, M. E. Goodrich, L. Ryan, R. LaCourse, R. J. North, The relative importance of T cell subsets in immunity and immunopathology of airborne Mycobacterium tuberculosis infection in mice. *J Exp Med* **193**, 271-280 (2001).
33. J. D. Yang *et al.*, Mycobacterium tuberculosis-specific CD4+ and CD8+ T cells differ in their capacity to recognize infected macrophages. *PLoS Pathog* **14**, e1007060 (2018).
34. T. Cheng, J. Y. Kam, M. D. Johansen, S. H. Oehlers, High content analysis of granuloma histology and neutrophilic inflammation in adult zebrafish infected with Mycobacterium marinum. *Micron* 10.1016/j.micron.2019.102782 (2019).
35. A. Bernut *et al.*, Deciphering and Imaging Pathogenesis and Cording of Mycobacterium abscessus in Zebrafish Embryos. *J Vis Exp* 10.3791/53130 (2015).
36. M. D. Johansen *et al.*, Mycobacterium marinum infection drives foam cell differentiation in zebrafish infection models. *Dev Comp Immunol* **88**, 169-172 (2018).

Figure Legends

Figure 1: *M. abscessus* establishes chronic infection in adult zebrafish.

A. Enumeration of CFUs from adult zebrafish infected with either the R or the S variant of *M. abscessus*.

B. Gene expression analysis of zebrafish *interleukin 1b*.

C. Gene expression analysis of zebrafish *tumor necrosis factor*.

D. Examples of R variant *M. abscessus*-Tdtomato lesions in 2 wpi *TgBAC(tnfa:GFP)*^{pd1028} adult zebrafish.

E. Example of S variant *M. abscessus*-Tdtomato lesions in 4 wpi *TgBAC(tnfa:GFP)*^{pd1028} adult zebrafish.

Filled arrowheads indicate organised necrotic granulomas with strong *tnfa* expression marked by GFP, empty arrowheads indicate loose *M. abscessus* lesions with elevated *tnfa* promoter induction. Scale bars indicate 200 μm.

Statistical tests by one-way ANOVA with Tukey's multiple comparisons test. Data is pooled from 10 animals across 2 independent experiments.

Figure 2: *M. abscessus* R infection causes progressive granulomatous pathology.

A. Stereotypical unorganised granuloma in a 2 wpi adult zebrafish infected with the R variant of *M. abscessus* expressing Tdtomato. Scale bar indicates 100 μm.

B. i. Stereotypical organised granuloma in a 2 wpi adult zebrafish infected with R *M. abscessus*-Tdtomato and ii. Higher magnification image of granuloma wall. Arrowheads indicate epithelised macrophage nuclei surrounding the mycobacterial core. Scale bar indicates 100 μm.

C. Example of a very large abscess-like granuloma in a 2 wpi adult zebrafish infected with R *M. abscessus*-Tdtomato measuring approximately 600 μm in diameter. Scale bar indicates 200 μm.

D. Example of Oil Red O-stained very large abscess-like granuloma in a 2 wpi adult zebrafish infected with R *M. abscessus*. Arrowheads indicate Oil Red O-positive foamy macrophages surrounding the mycobacterial core. Scale bar indicates 200 μm.

E. Quantification of granuloma organisation in adult zebrafish infected with R *M. abscessus*. Data is pooled from 2 animals per timepoint.

F. Quantification of bacterial burden stratified by granuloma organisation in adult zebrafish infected with R *M. abscessus*. Data is pooled from 2 animals per timepoint, statistical testing by Chi-squared test.

Figure 3: *M. abscessus* S infection causes delayed progressive granulomatous pathology.

A. Examples of S *M. abscessus*-Tdtomato lesions from 2 wpi adult zebrafish. i. *M. abscessus* growing free, external to peritoneal organs. ii. Stereotypical example of unorganised cellular granulomas around sites of sparse *M. abscessus* infection.

B. i. Stereotypical large granuloma found in 4 wpi adult zebrafish infected with S *M. abscessus*-Tdtomato. Note lack of punctate bacterial fluorescence in the core of the granuloma compared to loose bacteria to the right. ii. Example of Oil Red O-stained large granuloma in 4 wpi adult zebrafish infected with S *M. abscessus*. Note lack of lipid staining in the rim of the granuloma compared to R infection.

C. i. Quantification of granuloma organisation in adult zebrafish infected with S *M. abscessus*. ii. Quantification of bacterial burden stratified by granuloma organisation in adult zebrafish infected with S *M. abscessus*. Data is pooled from at least 2 animals per timepoint, statistical testing by Chi-squared test.

Figure 4: T cells are necessary to control R but not S *M. abscessus* infection.

A. Examples of T cell recruitment to granulomas in 2 wpi *TgBAC*(*lck*:*EGFP*)^{vcc4} adult zebrafish infected with R *M. abscessus*-Tdtomato . i. Example of an unorganised granuloma. ii. Example of an organised granuloma. iii. Example of a very large abscess-like granuloma. Scale bars indicate 100 μm.

B. Example of lack of T cell recruitment to S *M. abscessus*-Tdtomato in 2 wpi *TgBAC*(*lck*:*EGFP*)^{vcc4} adult zebrafish. Scale bar indicates 100 µm.

C. Survival analysis of WT and lck-/-^{sa410} adult zebrafish infected with R or S *M. abscessus*.

D. Enumeration of CFUs from 2 wpi WT and lck-/-^{sa410} adult zebrafish infected with R *M. abscessus*. Statistical testing by T-test.

E. Enumeration of CFUs from 2 wpi WT and lck-/-^{sa410} adult zebrafish infected with S *M. abscessus*. Statistical testing by T-test.

Figure 5: S *M. abscessus* has an *in vivo* survival advantage over R *M. abscessus* during chronic infection.

A. Schema outlining mixed infection experiment.

B. Ratio of R:S CFUs recovered from WT adult zebrafish infected with a mixture of differentially labelled R and S variant *M. abscessus*.

C. Enumeration of CFUs from the three groups of WT adult zebrafish outlined in panel A. Data is pooled from two replicates, statistical testing by ANOVA.

D. Representative images of granuloma from adult zebrafish infected with a mixture of R expressing Wasabi and S expressing Tdtomato *M. abscessus*.

E. Enumeration of CFUs from the three groups of lck-/-^{sa410} adult zebrafish outlined in panel A. Data is pooled from two replicates, statistical testing by ANOVA.

F. Ratio of R:S CFUs recovered from lck-/-^{sa410} adult zebrafish infected with a mixture of differentially labelled R and S variants.

Figure 1

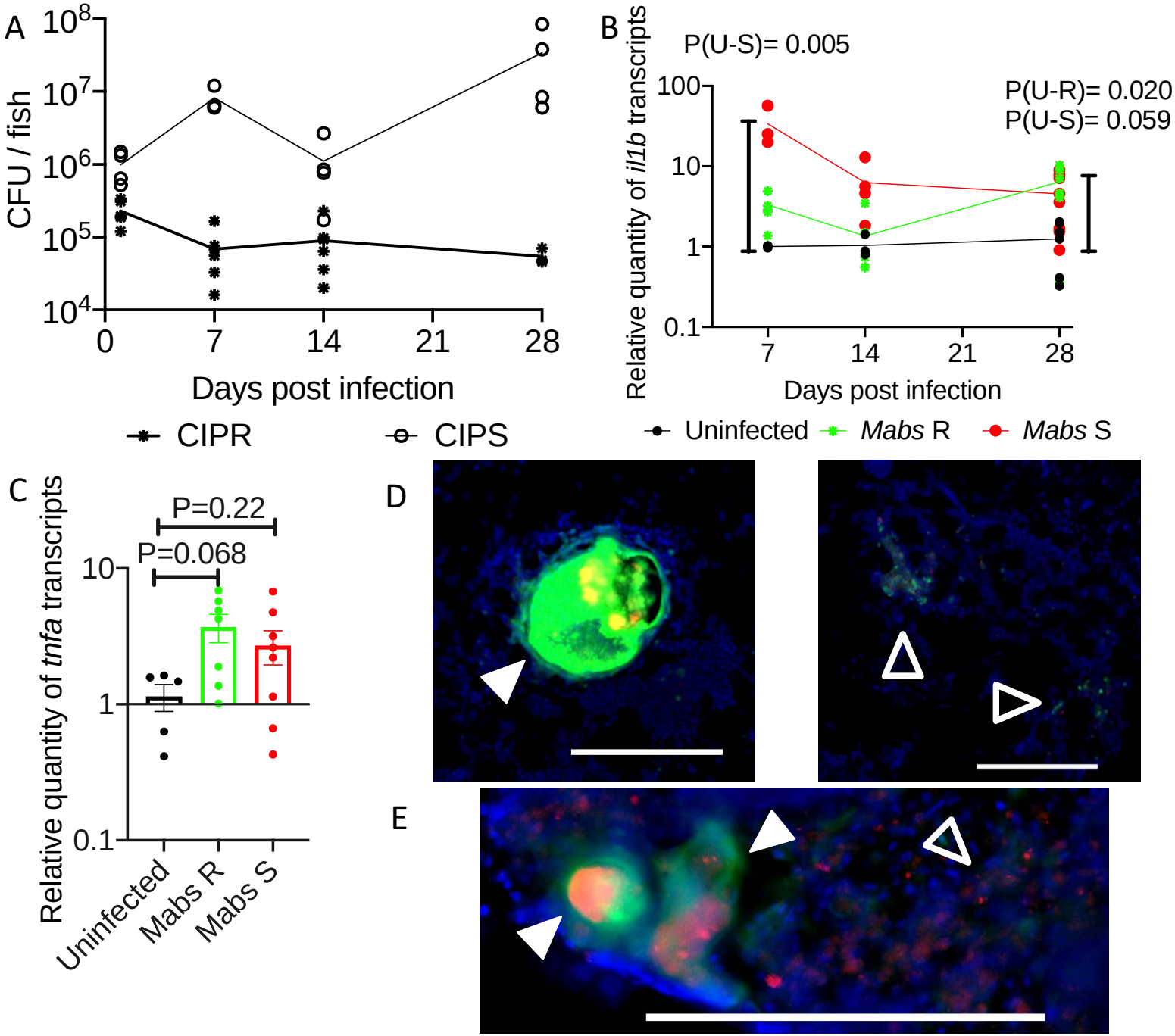
A
CFU / fish
10^8
10^7
10^6
10^5
10^4
0
7
14
21
28
Days post infection
CIPR
CIPS
B
Relative quantity of *il1b* transcripts
P(U-S)= 0.005
P(U-R)= 0.020
P(U-S)= 0.059
100
10
1
0.1
7
14
21
28
Days post infection
Uninfected
Mabs R
Mabs S
C
Relative quantity of *tnfa* transcripts
P=0.22
P=0.068
10
1
0.1
Uninfected
Mabs R
Mabs S
D
E

Figure 2

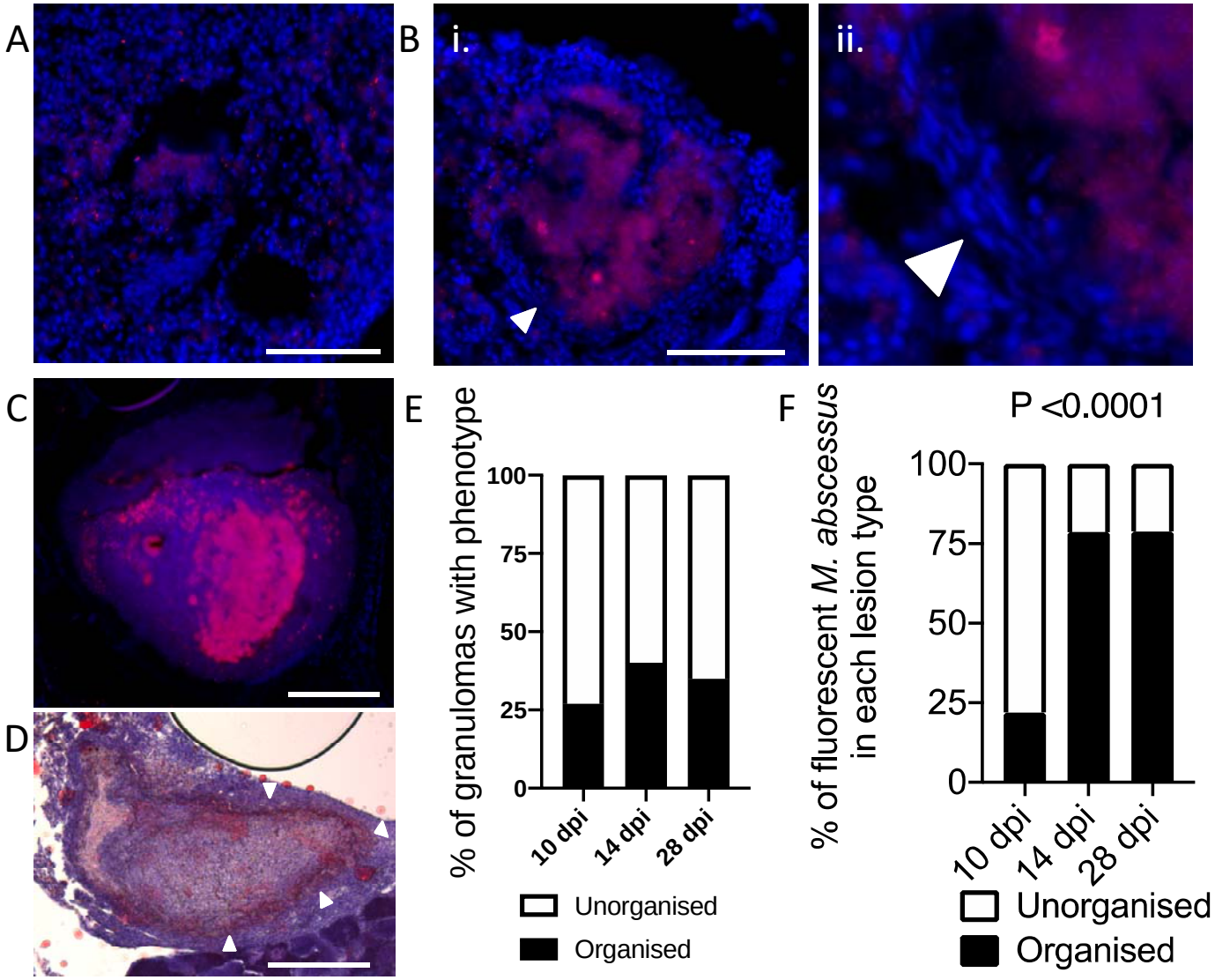
A
B
i.
ii.
C
D
E
% of granulomas with phenotype
100
75
50
25
0
10 dpi
14 dpi
28 dpi
Unorganised
Organised
F
P <0.0001
% of fluorescent M. abscessus in each lesion type
100
75
50
25
0
10 dpi
14 dpi
28 dpi
Unorganised
Organised

Figure 3

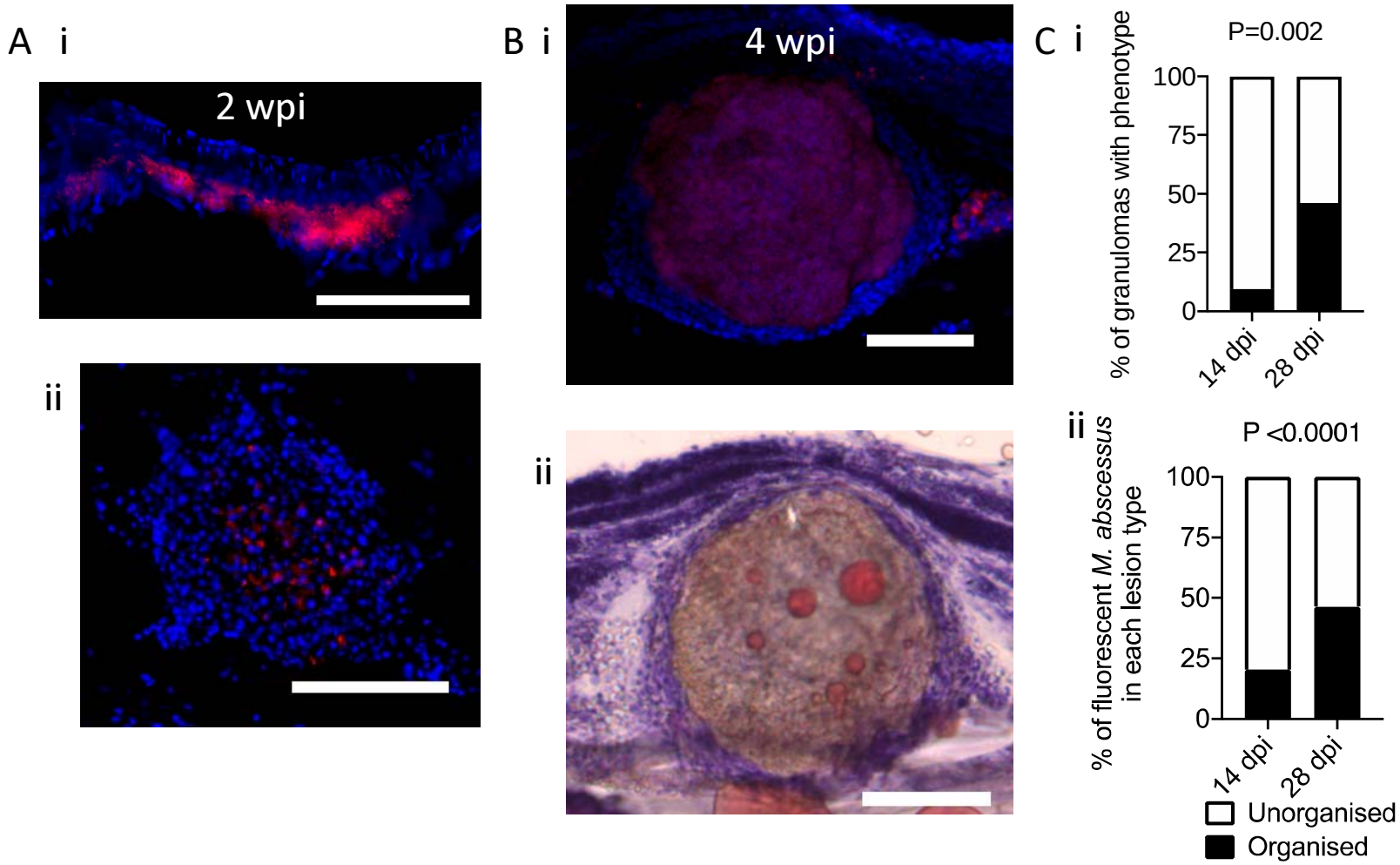
A i
2 wpi
ii
B i
4 wpi
ii
C i
P=0.002
% of granulomas with phenotype
100
75
50
25
0
14 dpi
28 dpi
ii
P <0.0001
% of fluorescent M. abscessus in each lesion type
100
75
50
25
0
14 dpi
28 dpi
Unorganised
Organised

Figure 4

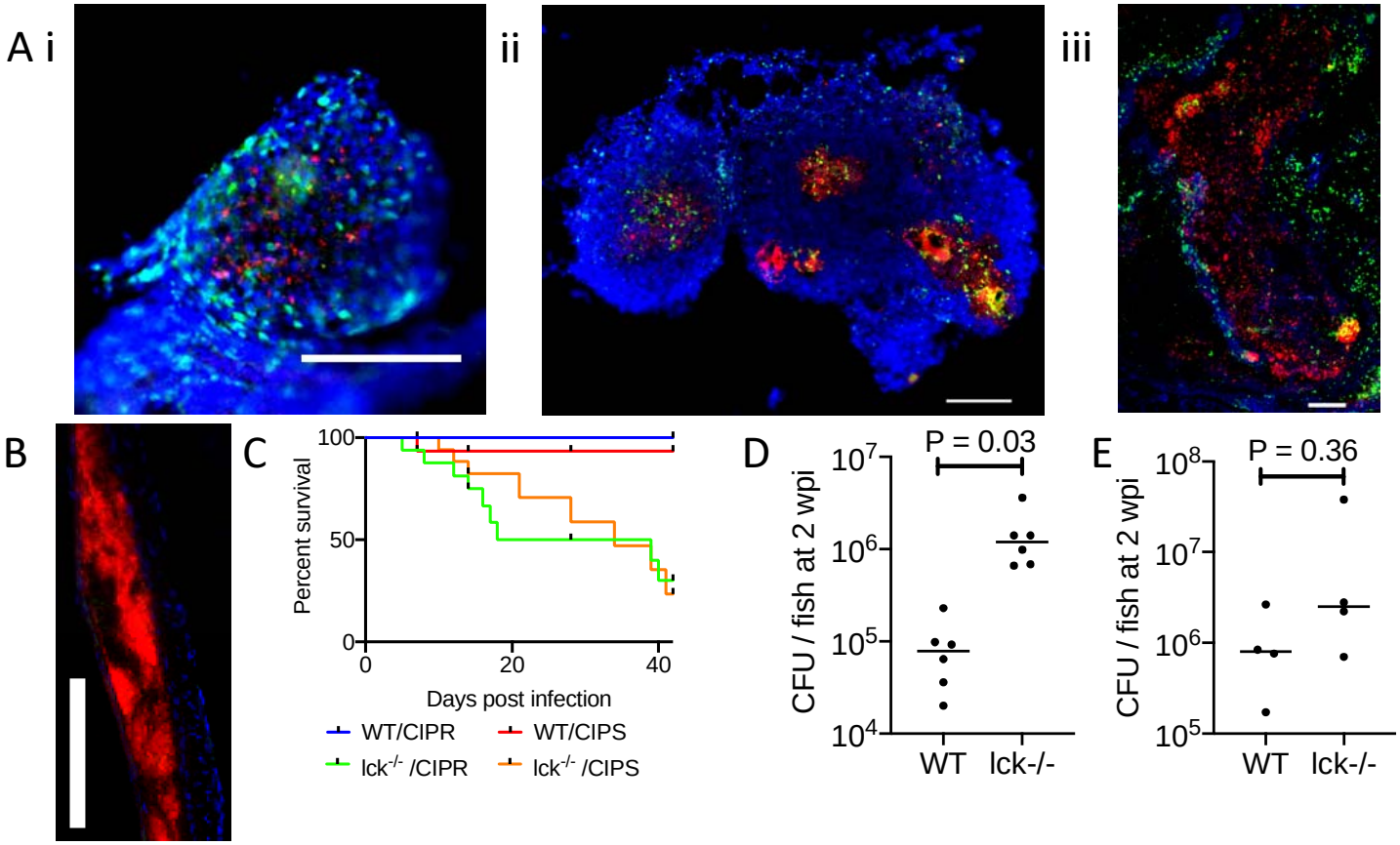
A i
ii
iii
B
C
Percent survival
100
50
0
0
20
40
Days post infection
WT/CIPR
WT/CIPS
lck-/- /CIPR
lck-/- /CIPS
D
P = 0.03
CFU / fish at 2 wpi
10^7
10^6
10^5
10^4
WT
lck-/-
E
P = 0.36
CFU / fish at 2 wpi
10^8
10^7
10^6
10^5
WT
lck-/-

Figure 5

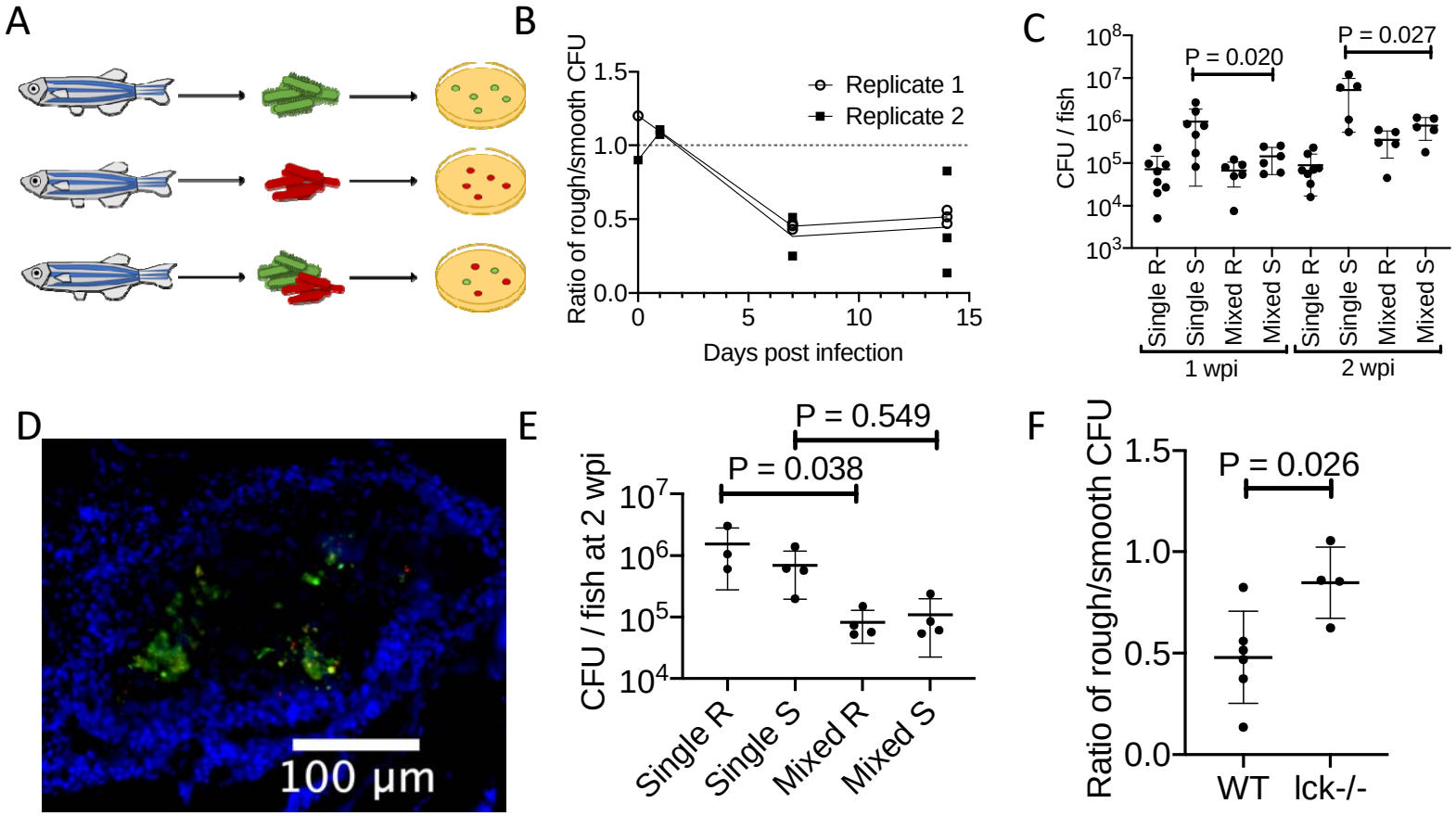
A
B
Ratio of rough/smooth CFU
1.5
1.0
0.5
0.0
0
5
10
15
Days post infection
Replicate 1
Replicate 2
C
CFU / fish
10^8
10^7
10^6
10^5
10^4
10^3
P = 0.020
P = 0.027
Single R
Single S
Mixed R
Mixed S
Single R
Single S
Mixed R
Mixed S
1 wpi
2 wpi
D
100 µm
E
CFU / fish at 2 wpi
10^7
10^6
10^5
10^4
P = 0.549
P = 0.038
Single R
Single S
Mixed R
Mixed S
F
Ratio of rough/smooth CFU
1.5
1.0
0.5
0.0
P = 0.026
WT
lck-/-
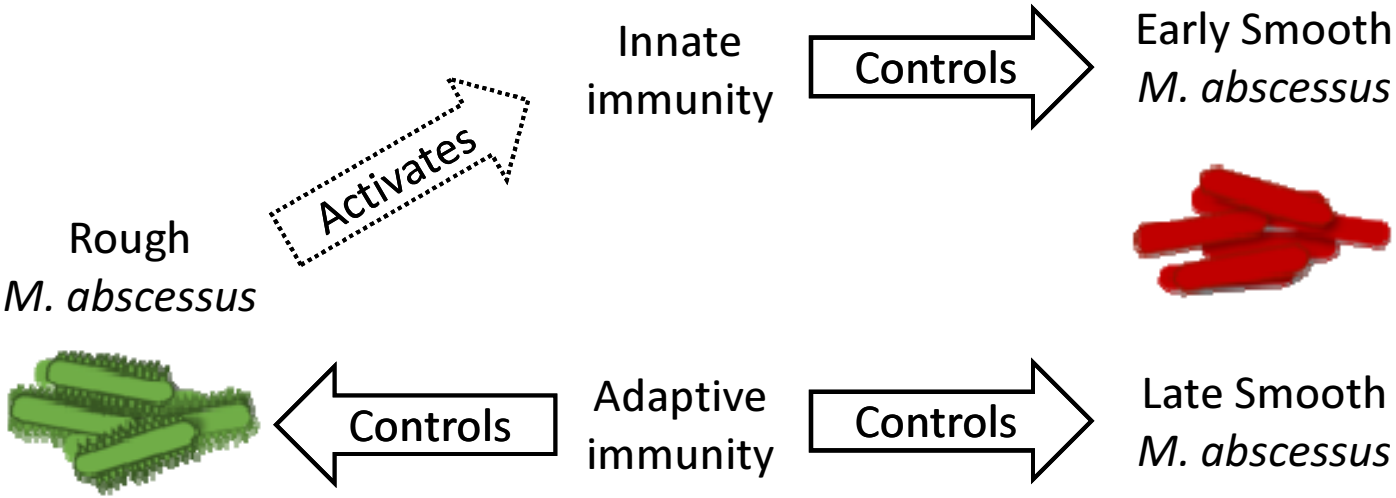
Graphical Abstract